Delft University of Technology

CIE5050-09 Additional Graduation Work

Analysis on the Heterogeneity of Proximity Resistance in Car Following

Student Quanyi Wang (5500869)

Supervisor Dr.ir.Simeon Calvert

Supervisor Yiru Jiao

January 20, 2023

TU Delft Delft University of Technology

1 Introduction

Car-following behaviour is a fundamental element for vehicle manoeuvre, which has been researched extensively over the past decades. The heterogeneity among driving behaviour has gained significant importance since some researchers argued that it might be relevant to capacity drop and traffic oscillations (S. Ossen & Hoogendoorn, 2011; Yuan et al., 2018; Makridis et al., 2022). Driver heterogeneity is usually distinguished into inter-driver heterogeneity and intra-driver heterogeneity. The inter-driver heterogeneity describes that different drivers may behave differently in the same environment because of different vehicle types and driving styles (S. Ossen & Hoogendoorn, 2011; Zhang et al., 2022). The stochasticity during decision-making is able to explain intra-driver heterogeneity, which potentially influences the variation of the same driver's behaviour under different conditions (Zhang et al., 2022). Therefore, it is meaningful to investigate heterogeneity to model human behaviour more accurately and thus improve the performance of traffic operation and control.

Due to the homogeneous behaviour assumption and ignorance of human factors, traditional mathematical car-following models and their extended models generally perform poorly in describing car-following behaviour, as well as traffic flow features (Han et al., 2022). The inherent heterogeneity among drivers makes it difficult to reproduce natural car-following behaviour accurately. Even though heterogeneity of human factors with normal distribution has been taken into account in some studies (Jiang et al., 2014; Tao et al., 2011; Zhu et al., 2020; Koutsopoulos & Farah, 2012), adding extra human-related parameters would result in higher complexity in model calibration (Saifuzzaman & Zheng, 2014; S. J. L. Ossen, 2008). Given the importance of the human factor in the decision-making process, heterogeneity characteristics of human factors could be analysed and used as decision variables when a new model needs to be proposed or to identify driver's features. Therefore, understanding the heterogeneity in car-following behaviour and modelling observed behaviours precisely has been attached to significant importance (Makridis et al., 2022).

With the development of Advanced Driver Assistant Systems (ADAS), such as Adaptive Cruise Control (ACC), Collaborative Adaptive Cruise Control(CACC), as well as Connected and Automated Vehicle Systems(CAVs), personalised systems with consideration of heterogeneity benefits for the improvement of the acceptance and use to customers. Particularly in the initial phase, customised ADAS and CAVS could bring a higher satisfactory experience to users, which could improve the trust of the system and willingness of future use (Qi & Guan, 2019; Sheng et al., 2022). Since it is crucial for drivers to feel comfortable within the implemented system, understanding the heterogeneity of driver space has enormous potential to develop better customised ADAS. However, there is a relatively small amount of literature about the impact of heterogeneity on driver space.

Drivers are always inclined to put themselves in their comfort zone (Peeta et al., 2005; Bärgman et al., 2015; Qi & Guan, 2019). The safe margins of drivers are not fixed numbers, and they are influenced by extensive factors from drivers' characteristics and external situations (Bärgman et al., 2015). Peeta et al. (2005) classified contributing factors for discomfort level into three categories: (1) socioeconomic characteristics; (2) situational factors; (3) latent driver's behaviour tendencies. Since discomfort feeling is related to a wide range of factors, quantitative representation is needed to investigate the heterogeneity's impacts.

This report investigates the impacts of heterogeneity on proximity resistance in terms of different traffic states, vehicle types and driving styles. It is expected to help build a personalised car-following model based on the probabilistic driver space inference.

The rest of the report is organised as figure 1 shows: Section 2 reviews the state-of-the-art work related to the heterogeneity of car-following behaviour and driver space. Section 3 introduces the inference procedure of driver space and proximity resistance. Section 4 presents data processing for driver clustering and proximity resistance calculation. Section 5 analyses the heterogeneity characteristics of proximity resistance among drivers in terms of different traffic states, vehicle types and driving styles. Finally, Section 6 conducts the conclusion and recommendation of potential future works.

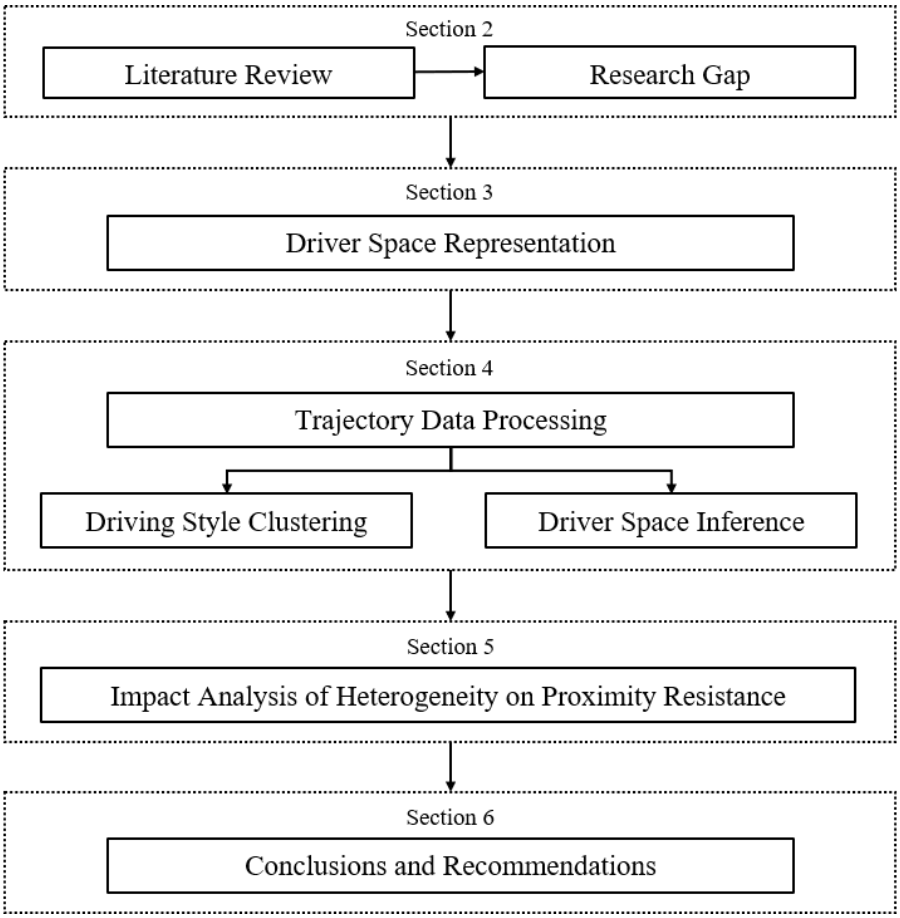

Figure 1: Research Framework

2 Literature Review

The interaction of driver-vehicle-environment combination can explain different characteristics of car-following behaviour (Han et al., 2022). Research about driver heterogeneity has been carried out over the past decades, and many researchers have approved the existence of heterogeneity for car-following behaviour. Liao et al. (2022); Sheng et al. (2022); Zhang et al. (2022) have noticed inter-driver differences in traffic-related parameters such as speed, distance headway, time headway and TTC for different driving styles. In addition, S. Ossen & Hoogendoorn (2011) identified the inter-heterogeneity caused by vehicle type that truck drivers drive with a more stable speed than car drivers. Except for inter-heterogeneity, latent intra-heterogeneity has also been researched by many researchers. Zhang et al. (2017) stated that drivers would adapt their driving styles under different traffic states. Different leader-follower combinations also result in heterogeneous car-following behaviour (S. Ossen & Hoogendoorn, 2011; W. Wang et al., 2021; Peeta et al., 2005), four types of state are divided into (1) car following car; (2) car following truck; (3) truck following truck; (4) truck following car. More detailed research about car-following behaviour in terms of driver, vehicle, and environmental factors can be found in these papers (Han et al., 2022; Saifuzzaman & Zheng, 2014).

Some indicators have been introduced to represent the discomfort feeling based on drivers' acceleration, such as "comfort index" (ratio between simulated acceleration and the sum of all vehicle's acceleration) (Paddan & Griffin, 2002) and "Jerk" (change rates of acceleration) (Zhu et al., 2020; K. Wang et al., 2022). However, discomfort feeling is affected by many factors, and only acceleration-related parameters are insufficient to attribute to it. Peeta et al. (2005) quantified discomfort grading from 1 to 5 through a stated preference survey with the individual socioeconomic characteristics (age, gender, education, household size) and the situational factors (weather, time of day, congestion level). This paper's discomfort index limitation is based on the stated preference survey, which might be inconsistent with the revealed car-following behaviour.

The concept of "comfort zone" was proposed by Näätänen & Summala (1974) based on work of Gibson & Crooks (1938). Discomfort will arise if the safety margin of a driver is intruded, which triggers drivers to react to the current situations to remain in their comfort zone (Summala, 2007). However, only a few researchers analysed the comfort zone using a quantitative representation. Bärgman et al. (2015) conducted a test-track experiment to quantify driver's comfort-zone boundaries in left-turn-across-path scenarios based on post-encroachment time (PET), lateral acceleration and self-reports of comfort and risk. In addition, Qi & Guan (2019) proposed a situational discomfort grading system based on the driver's situational reaction data from experiments. The discomfort is represented by acceleration value, and a larger absolute value indicates a stronger willingness to leave the current situation. However, none provided a quantitative representation of comfort zone using empirical data to analyse the heterogeneity in driving behaviour.

Similarly to comfort zone, Jiao et al. (2022) proposed "driver space" to reflect the transition between comfort and discomfort of drivers. Driver space is an area around a vehicle, and drivers will feel a rapid increase in discomfort when their space boundary is intruded. The response intensity of discomfort caused by spatial intrusion is represented by proximity resistance. Based on trajectory data, heterogeneity of driver space for the same drivers is observed depending on different relative speeds.

The discomfort is related to extensive factors, especially human-related factors, making it challenging to evaluate heterogeneity's impacts directly. Instead of discomfort level, the proximity resistance will be used in this report to reflect the discomfort response caused by the spatial intrusion.

3 Driver Space Representation

In this report, the concept and methodology of driver space representation are obtained from Jiao et al. (2022). Based on urban trajectory data, the accumulative density of infrequent presence surrounding vehicles is used to express two-dimensional driver space quantitatively. In this report, only longitudinal driver space is inferred, the lateral driver space made by lane-changing behaviour is not considered. Proximity resistance is not a probability density, its mathematical expression is shown in formula 1, which indicates that proximity resistance p is a function of x, r and β based on the condition of different relative speed. x represents the relative position between two vehicles; r denotes how far the driver space boundary is; β reflects how fast the discomfort transition is; r>0 and β >2. The distribution of proximity resistance is displayed in figure 2.

$$p(x|r,\beta) = exp(-|\frac{x}{r}|^{\beta}) \tag{1}$$

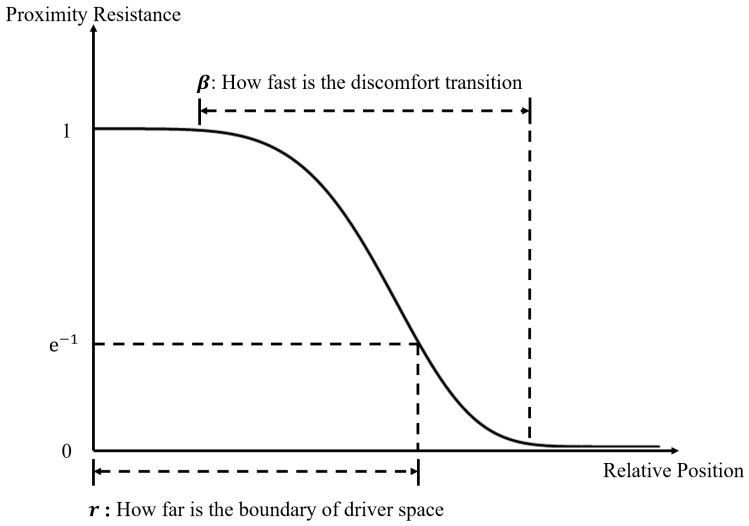

Figure 2: One-dimensional Driver Space with Parameters r and β

The inference of driver space mainly includes two steps: (1) Estimation of scale parameter r and shape parameter β for driver space; (2) Inference of proximity resistance based on the function of relative position. If there is a pair of ego vehicle i at x_i, y_i and preceding vehicle j at x_j, y_j. The likelihood of the presence of the preceding vehicles are in formula 2. Proximity resistance p_{ij} between vehicle i and j is inferred by maximising likelihood L until r and β converge, where β are estimated given r and r given β.

$$L = \prod_{j=1}^{n}[1 - p_{ij}(x_j|r,\beta)] \tag{2}$$

For more convenient computation, the sum of log-likelihood and $\epsilon = 10^{-4}$ are added to alleviate the bias of overly small r and β caused by minimal driver space. The final adjusted log-likelihood of the presence of n surrounding vehicles is in formula 3.

$$\ln(L) = \prod_{j=1}^{n}\ln[1 + \epsilon - p_{ij}(x_j|r,\beta)] \tag{3}$$

4 Data Processing

Three major steps will be carried out sequentially in the data processing stage to obtain the datasets for driver clustering and proximity resistance. Firstly, it is essential to determine the datasets that will be used to investigate the impacts of heterogeneity on proximity resistance. Secondly, driver clustering in terms of driving style will be performed through the K-means clustering method and visualised by the T-SNE approach. Meanwhile, the different driving characteristics of each cluster will be summarised. Thirdly, the quantitative drive space will be calculated based on the methodology described in Section 3. The detailed inference process of driving styles characteristics and proximity resistance is shown in figure 4.

4.1 HighD Dataset

In this study, HighD dataset is used for driving style clustering and proximity resistance inference. HighD (Krajewski et al., 2018) is a dataset including naturalistic vehicle trajectories recorded on German highways using a drone covering a road segment of about 420 m as shown in 3a. At six different locations around Cologne (3b), 60 recordings are made with an average duration of 17 minutes. In order to improve the data quality, resolution 4K camera recordings are only made during sunny and windless weather from 8 AM to 5 PM to reduce the influence of movements. In addition, state-of-the-art computer vision algorithms are applied to extract information like vehicle characteristics and manoeuvres at a frame rate of 25 Hz.

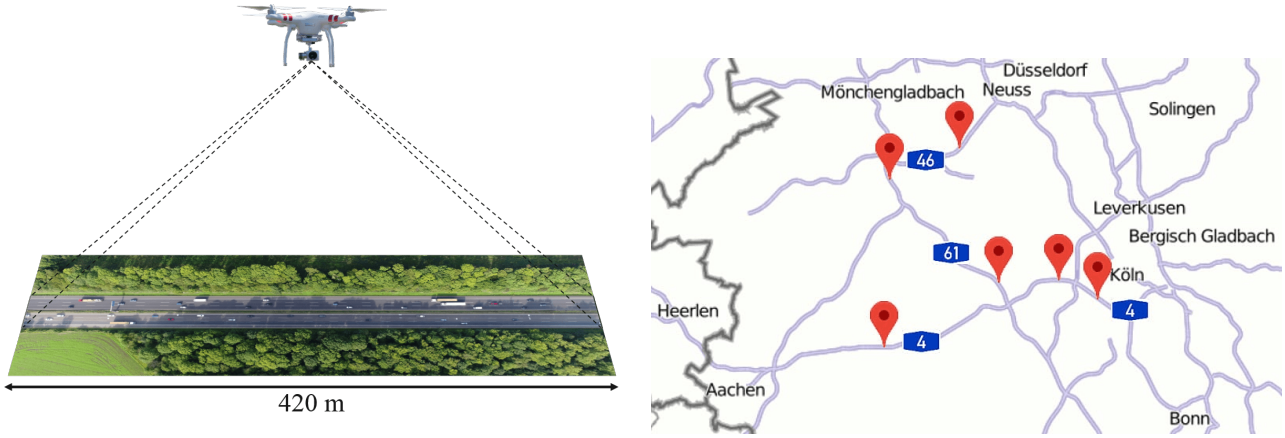

(a) Recording Setup of HighD Dataset

(b) Locations of Recordings in HighD Dataset

Figure 3: HighD Dataset (Krajewski et al., 2018)

The recordings information is summarised in Table 2 in Appendix. In order to reduce the influence of the external environment, it is better to choose recordings at the same location in the same driving direction. This report selected location 1 (37 recordings) because it has the largest dataset among 60 recordings. It has three lanes in each direction, and the speed limit is 120 km/h.

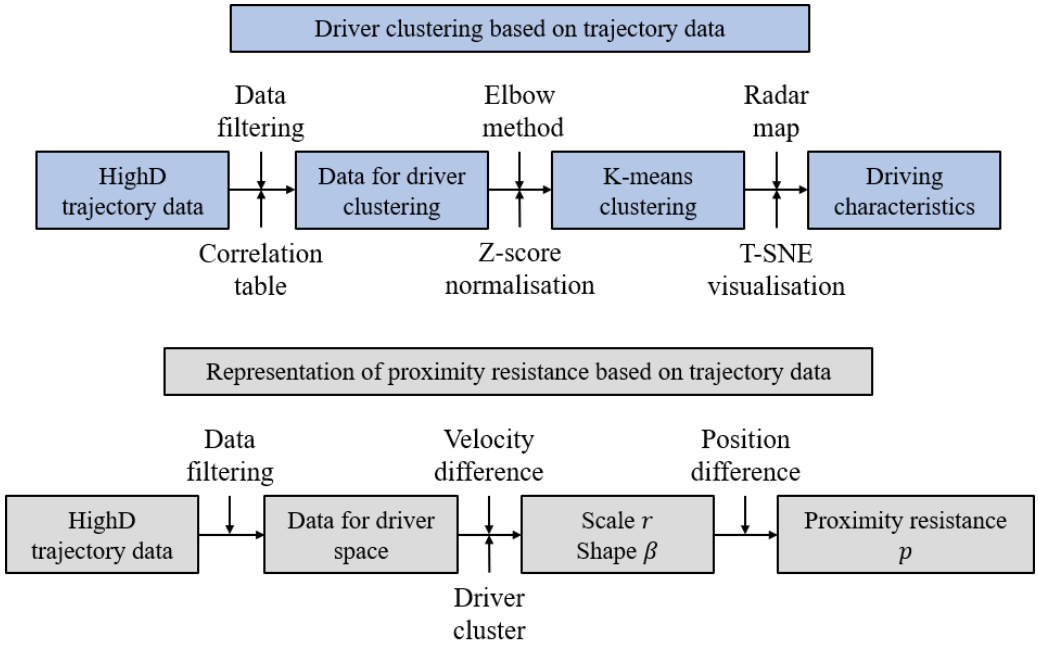

Figure 4: Overview of Data Processing

4.2 Driver Clustering

After selecting the dataset successfully, the next step is distinguishing different car-following driving styles. Trajectories should be filtered to ensure that drivers are in a steady car-following state, and therefore several constraints are set based on literature (Kurtc, 2020; W. Wang et al., 2021; Z. Wang et al., 2022):

- Exclude trajectories without preceding vehicle.
- Exclude trajectories with lane changes to avoid rapid velocity.
- Exclude the duration of trajectories less than 15s (375 frames) to make the characteristics of car-following be explained.
- Exclude distance headway larger than 150 m to guarantee the influence of the preceding vehicle.
- Change the Time-to-Collision(TTC) larger than 10s equal to 10s and do not take negative TTC into account when calculating.
- Add an additional indicator to reflect the driving stability: the ratio of constant speed duration compared to the duration of acceleration.

Before applying driver clustering, the correlation between variables of both cars and trucks like mean, min, max, std of velocity, acceleration, deceleration, dhw, thw, ttc, and duration ratio of constant speed will be made to decide which variables should be included for clustering, which is shown in figure 5. Afterwards, Elbow-method will be used to determine the cluster number after the z-score normalisation, and then the k-means methodology will be applied for clustering.

4.2.1 Correlation Table

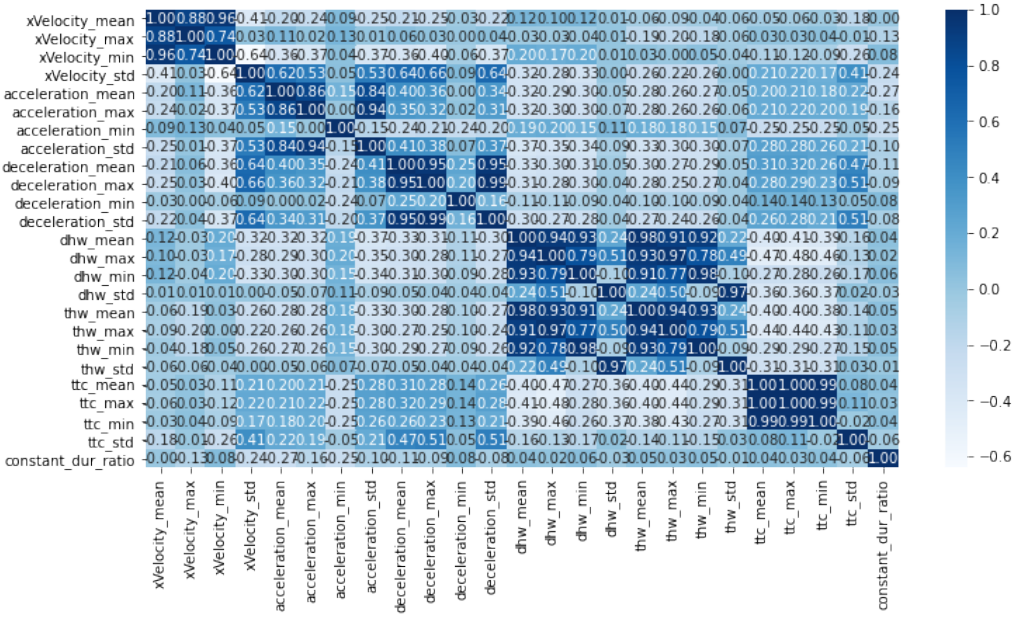

Figure 5: Correlation Table for the Whole Dataset

According to figure 5, it is noted that several groups of factors have a considerable correlation, which is summarised as follows.

- Mean, maximum and minimum of Velocity
- Mean, maximum and standard deviation of acceleration and deceleration
- Mean, maximum and minimum of distance headway and time headway
- Mean, maximum and minimum of distance headway and the counterparts s of time headway
- Mean, maximum and minim of TTC

This step aims to select factors that help to cluster precisely and explain the characteristics powerfully, so factors can be kept despite having a high correlation with others. This report uses the mean value to reflect the driving magnitude, and the standard deviation value represents the stability. Since distance headway and time headway have a significant correlation relationship, thus only distance headway will be used. The minimum distance headway and TTC are used to reflect the risky behaviour in the collision. The ratio of constant speed duration can also reflect the stability of drivers. Figure 6 illustrates the final correlation table for cars and trucks.

4.2.2 K-means Clustering

The Elbow method is commonly used to find the optimal number of clusters in the K-means clustering algorithm. The sharp decrease is observed before the actual clustering number 2 in Figure 7. Thus two clusters are determined for both cars and trucks. Figure 8 visualises the characteristics difference of driving styles for each driver cluster. In addition, the T-distributed Stochastic Neighbour Embedding (T-SNE) algorithm (Van der Maaten & Hinton, 2008) is used to reduce the dimension of the high-dimensional clustering indicators, which is visualised in figure 9.

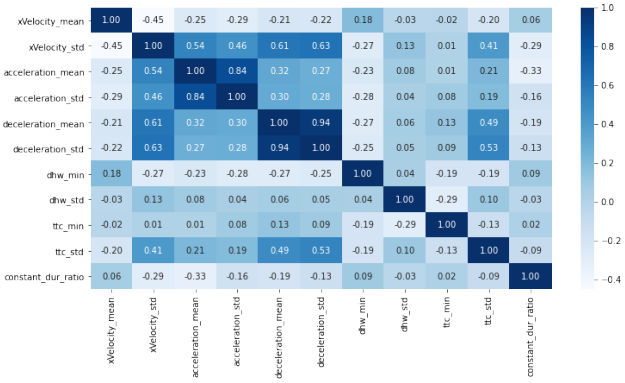

(a) Correlation Table for Car Dataset

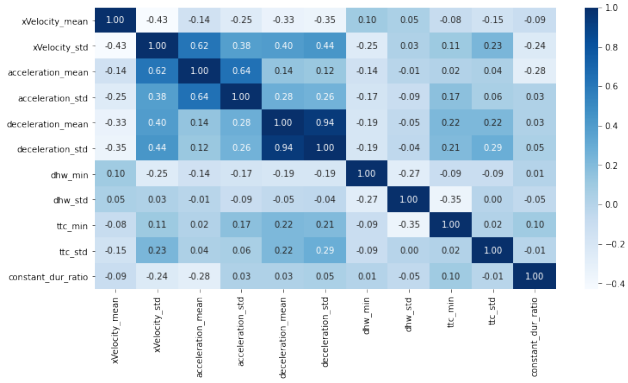

(b) Correlation Table for Truck Dataset

Figure 6: Correlation Tables for Drivers

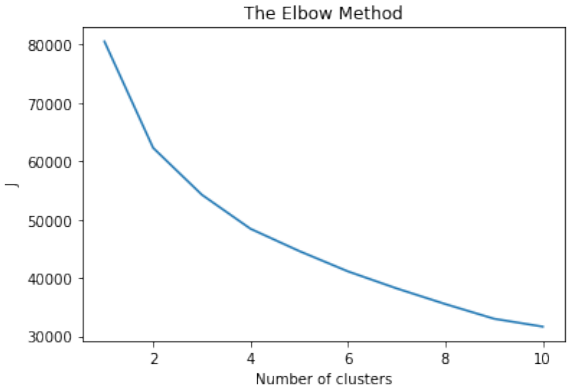

(a) The Elbow Method for Car

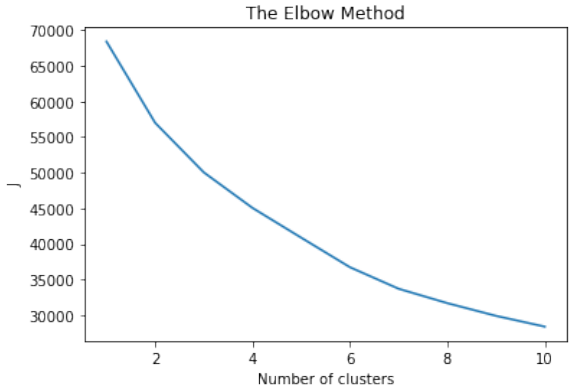

(b) The Elbow Method for Truck

Figure 7: The Elbow Method for Cars and Trucks

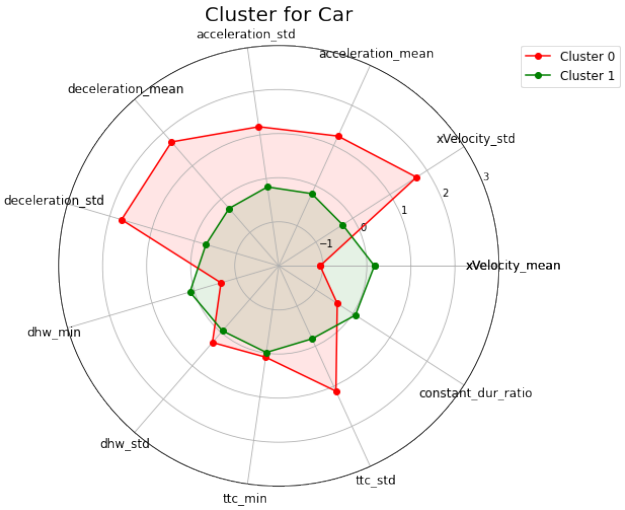

(a) Driving Style for Car Drivers

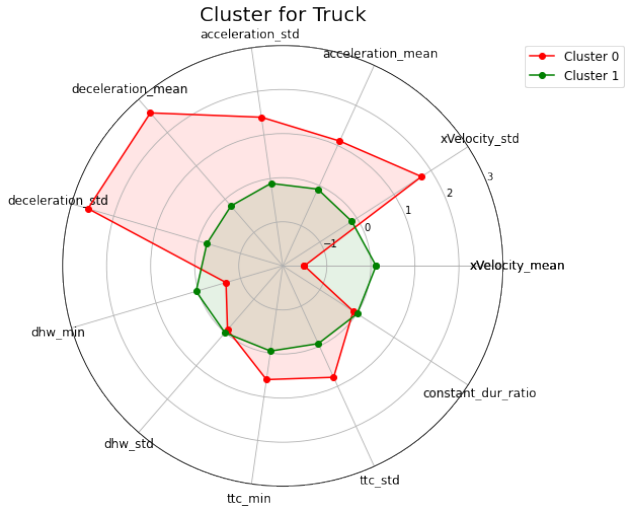

(b) Driving Styles for Truck Drivers

Figure 8: Radar Map for Driving Styles

4.2.3 TSNE Visualisation

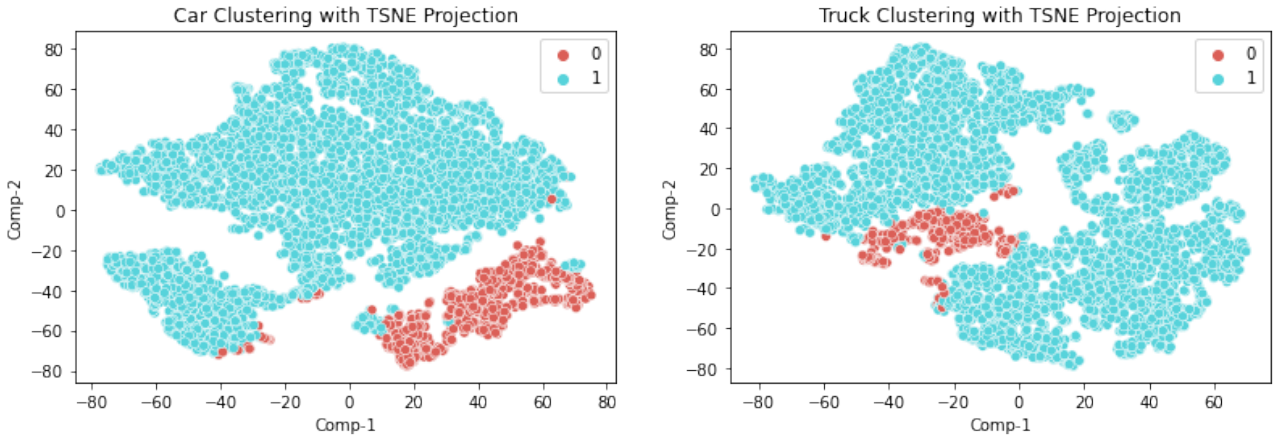

(a) Car Clustering with TSNE Projection

(b) Truck Clustering with TSNE Projection

Figure 9: Driver Clustering with TSNE Projection

According to figure 8, cluster 0 is defined as "unstable drivers" and cluster 1 as "stable drivers" in this report. After clustering drivers based on the indicators of driving styles, the information on drivers with different driving styles is listed in Table 3 in Appendix. Therefore, 86.1% stable car drivers, 13.9% unstable car drivers, 92.8% stable truck drivers and 7.2% unstable truck drivers are observed from the dataset, which will be used as driver space inference in the next step.

4.2.4 Characteristics of Driving Style

From the perspective of driving style, stable drivers have steady performance in all indicators. In contrast, unstable drivers tend to have unstable car-following behaviours even though they drive more slowly, which can be proven by the higher standard deviation of velocity, acceleration, deceleration, distance headway, TTC, and lower constant speed duration ratio. In addition, unstable drivers have more intense behaviour because of the large magnitude of acceleration and deceleration, which means they are more often to slam on the brake and accelerator pedals. Furthermore, even though stable drivers keep lower minimum distance headway, the lower minimum TTC reflect more risky car-following behaviours to a collision.

4.3 Driver Space Inference

The dataset for driver space inference should include both ego vehicle and preceding vehicle information to calculate the proximity resistance for each cluster at each frame. The r and β in different relative velocities for each cluster will be calculated through the driver space inference algorithm (Jiao et al., 2022). Afterwards, proximity resistance can be calculated based on the relative position, r, and β at each frame by using equation 1. The final processed dataset consists of driver cluster and car-following information like vehicle type, vehicle size, Lane ID, speed difference, distance headway and proximity resistance at each frame.

5 Heterogeneity Analysis

In this section, because the sample size of cars and trucks is different in the two traffic states, the impacts of heterogeneities on proximity resistance will be analysed using a density histogram. According to the figure 2, the corresponding proximity resistance at the boundary of a driver space r is e^{-1} in Section 3, which will be used to divide the driver state into non-intrusive (smaller than e^{-1}) and intrusive (larger than e^{-1}). In addition, Mahajan (2019) used the Gaussian Mixture algorithm on aggregated density and speed to differentiate the traffic state using HighD dataset. Because of the same dataset and road layout used in this paper, the boundary value of the average flow speed 70 km/h is also applied to analyse the impacts of traffic states on proximity resistance. Table 1 gives the overview of driver space based on Table 4 in Appendix. Figure 10 illustrates the driver space boundaries for different drivers under different relative speeds, drivers with larger r need larger driving space, which will be used to explain the potential reasons for heterogeneity's impacts on proximity resistance. In addition, $index$ in equation 4 represents the area where proximity resistance over the threshold value e^{-1}, which helps in understanding the heterogeneity more efficiently.

Table 1: Summary of Driver Space Intrusion Information

	Free-Flow State				Congested State			
	Car		Truck		Car		Truck	
	U	S	U	S	U	S	U	S
Non-intrusive	96.6%	94.1%	94.2%	95.9%	90.7%	89.8%	93.3%	97.2%
Intrusive	3.4%	5.9%	5.8%	4.1%	9.3%	10.2%	6.7%	2.8%

* Cluster U: unstable Drivers; Cluster S: stable Drivers

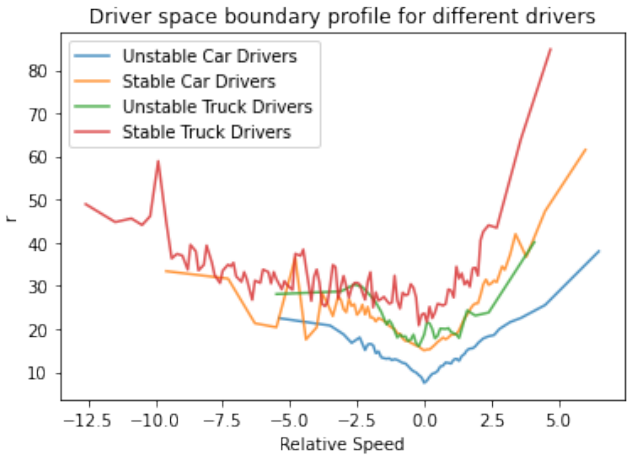

Figure 10: Driver Space Boundary Profile for Different Drivers

$$index = \int_{e^{-1}}^{1} p(pr) \cdot pr \tag{4}$$

5.1 Impacts of Traffic States on Proximity Resistance

Based on figure 11, except for the stable truck drivers, drivers experience higher proximity resistance in the congested state than in the free-flow state. It can be explained that drivers have to keep a smaller

distance headway between the preceding vehicles in the congested state than in the free-flow state. In contrast, it is interesting that stable truck drivers have higher proximity resistance in the free-flow state than in the congested state. It might be because traffic states might not affect the performance of stable truck drivers, and they might always stay close to the preceding vehicles in both states. Another potential reason is insufficient samples of stable truck drivers in the congested state. Furthermore, it is meaningful to observe that driving styles have a more significant impact on the proximity resistance of truck drivers than car drivers.

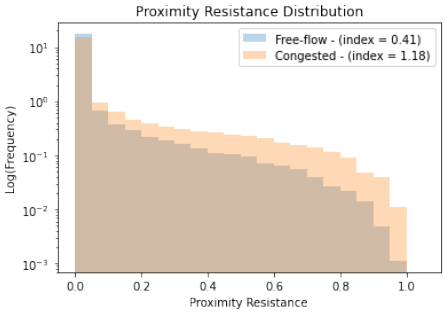

(a) Unstable Car Drivers

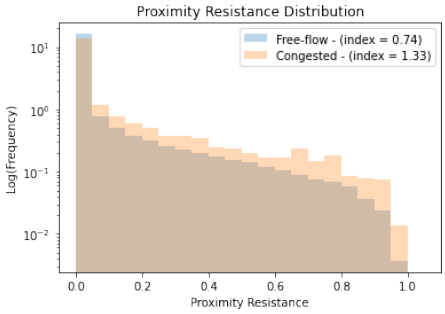

(b) Stable Car Drivers

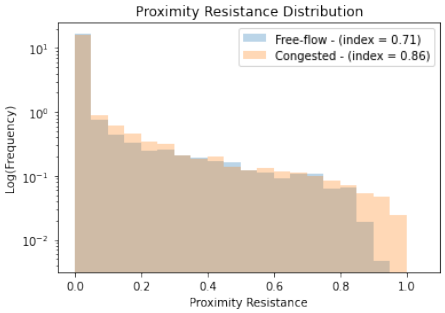

(c) Unstable Truck Drivers

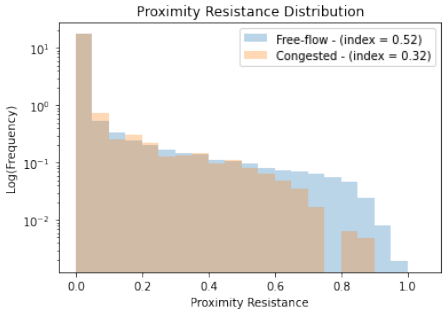

(d) Stable Truck Drivers

Figure 11: Impacts of Traffic States on Proximity Resistance

5.2 Impacts of Vehicle Types on Proximity Resistance

Based on figure 12, higher proximity resistance is experienced by unstable truck drivers than unstable car drivers in the free-flow state, which might not be the case in reality. Since unstable truck drivers need a larger driving space than unstable car drivers based on figure 10. In the congested state, car drivers are more likely to intrude driver space of others than truck drivers because truck drivers need larger driving space than car drivers and tend to keep a larger distance between the preceding vehicles to avoid a rear collision.

5.3 Impacts of Driving Styles on Proximity Resistance

Based on figure 13, stable car divers experience higher proximity resistance than unstable car drivers in both states. It means that stable car drivers are more likely to intrude driver space of others than unstable car drivers, which might not align with reality. In contrast, stable truck drivers have less proximity resistance than unstable truck drivers in both states, which can be explained by the larger driving space needed for stable truck drivers than unstable truck drivers based on figure 10, and stable truck drivers tend to keep larger distance headway between the preceding vehicles. Another interesting finding is that traffic state impacts truck drivers more than car drivers.

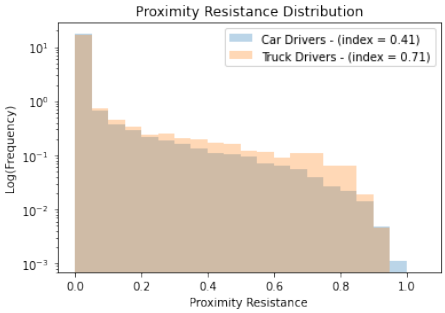

(a) Free-flow Unstable Drivers

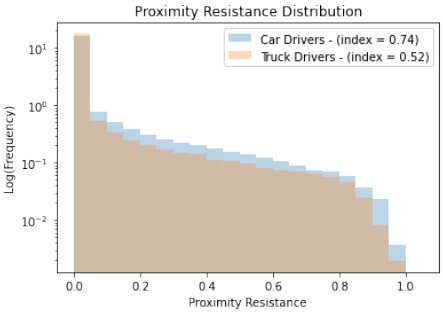

(b) Free-flow Stable Drivers

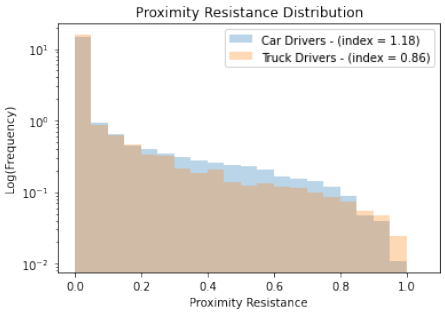

(c) Congested Unstable Drivers

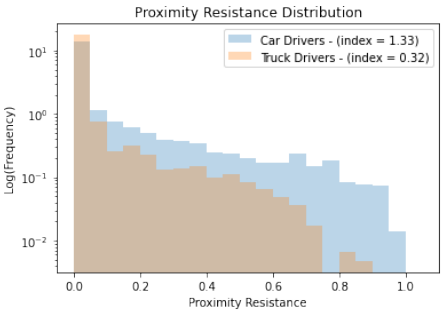

(d) Congested Stable Drivers

Figure 12: Impacts of Vehicle Types on Proximity Resistance

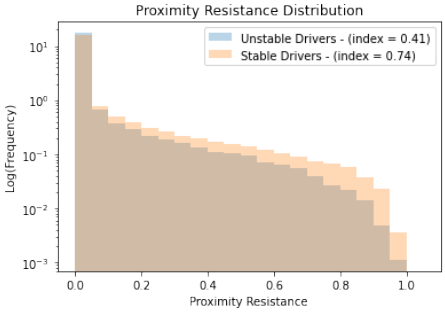

(a) Free-flow Car Drivers

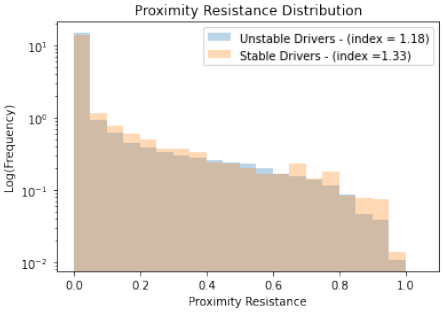

(b) Congested Car Drivers

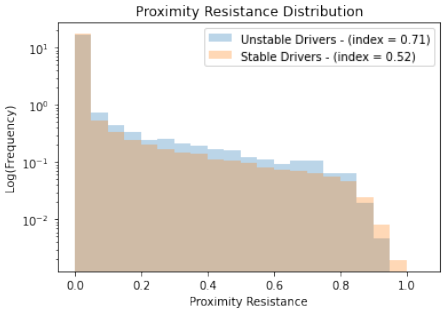

(c) Free-flow Truck Drivers

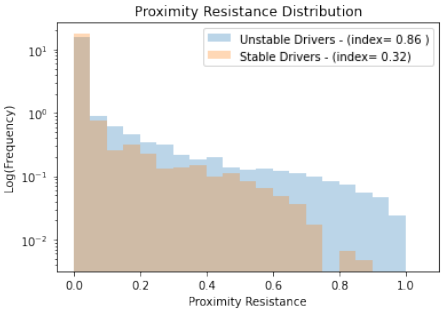

(d) Congested Truck Drivers

Figure 13: Impacts of Driving Styles on Proximity Resistance

6 Conclusion

This report aims to analyse the impacts of heterogeneity on driver's proximity resistance, which can be beneficial for developing personalised car-following models. HighD dataset was processed to make a distinction between driving styles for car and truck drivers and infer their frame-dependent proximity resistance. The K-means algorithm clustered the driving styles based on the selected performance indicators of car-following behaviours. Radar maps were used to compare the heterogeneous driving styles. After successfully inferring the proximity resistance for each driver at each frame, the impacts of inter-heterogeneity (driving styles, vehicle types) and intra-heterogeneity (traffic states) on proximity resistance were analysed. The main findings are shortly summarised below:

- Except for the stable truck drivers, drivers always experience higher proximity resistance in the congested state than in the free-flow state.
- Except for the unstable drivers in the free-flow state, truck drivers are experience lower proximity resistance than car drivers.
- Stable car drivers experience higher proximity resistance than unstable car drivers, while stable truck drivers experience lower proximity resistance than unstable truck drivers.
- Traffic states have a larger impact on the proximity resistance of truck drivers than car drivers.
- Driving styles have a larger impact on the proximity resistance of truck drivers than car drivers.

However, this report has several limitations that cannot be ignored. Firstly, the one-dimensional proximity resistance representation is a simplified version of two-dimensional driver space in Jiao et al. (2022). The influence of surrounding vehicles on the other lanes and lane-changing behaviour are not taken into account, which might cause overestimated proximity resistance experienced by drivers. Secondly, the boundary value of average speed for dividing free-flow and congested conditions was obtained from paper Mahajan (2019), which might not be the most accurate and suitable value for this report. Moreover, there are several observations about truck drivers that might contrasts with the reality because of insufficient samples, which also needs further improvement.

Therefore, it is recommended to apply a two-dimensional proximity resistance considering the influence of surrounding vehicles and lane-changing behaviours for more precise representation. In addition, a fundamental diagram based on trajectory data can be constructed to distinguish free-flow and congested states more accurately.Moreover, future work could study the quantitative impacts of heterogeneity on proximity resistance to better understand the extent of the effects. Furthermore, conducting an in-depth study on the heterogeneity of proximity resistances at different bottlenecks is also worthwhile. Last but not least, a car-following model incorporating the proximity resistance index could be proposed.

Appendix

Table 2: Summary of HighD Recordings Information

Location Id	Number of Recordings	Number of Lanes	Number of Cars	Number of Trucks	Speed Limits (km/h)
1	37	3+3	69751	16211	120
2	3	2+2	2400	674	No speed limit
3	3	3+3	2710	1037	130
4	4	3+3	3799	952	No speed limit
5	10	2+2	8192	1887	No speed limit
6	3	4+3	2287	616	120

Table 3: Number of Driving Style Clustering Information

	Car	Truck
Stable Driver	6237	5570
Unstable Driver	1005	451
Total	7242	6221

Table 4: Summary of Driver Space Intrusion Infomration

	Free-Flow State				Congested State			
Unit:Frame	Car		Truck		Car		Truck	
Cluster	U	S	U	S	U	S	U	S
Non-intrusive	240718	2084778	116097	1729366	219843	106505	65212	32520
Intrusive	8516	130055	7098	74796	22655	12141	4647	944

References

Bärgman, J., Smith, K., & Werneke, J. (2015). Quantifying drivers' comfort-zone and dread-zone boundaries in left turn across path/opposite direction (ltap/od) scenarios. *Transportation Research Part F: Traffic Psychology and Behaviour*, *35*, 170–184. Retrieved from https://doi.org/10.1016/j.trf.2015.10.003

Gibson, J. J., & Crooks, L. E. (1938). A theoretical field-analysis of automobile-driving. *The American journal of psychology*, *51*(3), 453–471. Retrieved from https://psycnet.apa.org/doi/10.2307/1416145

Han, J., Wang, X., & Wang, G. (2022). Modeling the car-following behavior with consideration of driver, vehicle, and environment factors: a historical review. *Sustainability*, *14*(13), 8179. Retrieved from https://doi.org/10.3390/su14138179

Jiang, R., Hu, M.-B., Zhang, H., Gao, Z.-Y., Jia, B., Wu, Q.-S., ... Yang, M. (2014). Traffic experiment reveals the nature of car-following. *PloS one*, *9*(4), e94351. Retrieved from https://doi.org/10.1371/journal.pone.0094351

Jiao, Y., Calvert, S. C., van Cranenburgh, S., & van Lint, H. (2022). Probabilistic representation for driver space and its inference from urban trajectory data. *Available at SSRN 4187513*. Retrieved from https://dx.doi.org/10.2139/ssrn.4187513

Koutsopoulos, H. N., & Farah, H. (2012). Latent class model for car following behavior. *Transportation research part B: methodological*, *46*(5), 563–578. Retrieved from https://doi.org/10.1016/j.trb.2012.01.001

Krajewski, R., Bock, J., Kloeker, L., & Eckstein, L. (2018). The highd dataset: A drone dataset of naturalistic vehicle trajectories on german highways for validation of highly automated driving systems. In *2018 21st international conference on intelligent transportation systems (itsc)* (p. 2118-2125). Retrieved from 10.1109/ITSC.2018.8569552

Kurtc, V. (2020). Studying car-following dynamics on the basis of the highd dataset. *Transportation research record*, *2674*(8), 813–822. Retrieved from https://doi.org/10.1177/0361198120925063

Liao, Y., Yu, G., Chen, P., Zhou, B., & Li, H. (2022). Modelling personalised car-following behaviour: a memory-based deep reinforcement learning approach. *Transportmetrica A: Transport Science*, 1–29. Retrieved from https://doi.org/10.1080/23249935.2022.2035846

Mahajan, V. (2019). Real-time driving intention prediction and crash risk estimation from naturalistic driving data using machine learning. Retrieved from https://mediatum.ub.tum.de/doc/1523133/file.pdf

Makridis, M. A., Anesiadou, A., Mattas, K., Fontaras, G., & Ciuffo, B. (2022). Characterising driver heterogeneity within stochastic traffic simulation. *Transportmetrica B: Transport Dynamics*, 1–19. Retrieved from https://doi.org/10.1080/21680566.2022.2125458

Näätänen, R., & Summala, H. (1974). A model for the role of motivational factors in drivers' decision-making∗. *Accident Analysis & Prevention*, *6*(3-4), 243–261. Retrieved from https://doi.org/10.1016/0001-4575(74)90003-7

Ossen, S., & Hoogendoorn, S. P. (2011). Heterogeneity in car-following behavior: Theory and empirics. *Transportation research part C: emerging technologies*, *19*(2), 182–195. Retrieved from https://doi.org/10.1016/j.trc.2010.05.006

Ossen, S. J. L. (2008). Longitudinal driving behavior: theory and empirics. Retrieved from http://repository.tudelft.nl/assets/uuid:fe2291ad-185b-4813-a518-e13ed31994a3/trail_ossen_20080916.pdf

Paddan, G., & Griffin, M. (2002). Evaluation of whole-body vibration in vehicles. *Journal of sound and vibration*, *253*(1), 195–213. Retrieved from https://doi.org/10.1006/jsvi.2001.4256

Peeta, S., Zhang, P., & Zhou, W. (2005). Behavior-based analysis of freeway car–truck interactions and related mitigation strategies. *Transportation Research Part B: Methodological*, *39*(5), 417–451. Retrieved from https://doi.org/10.1016/j.trb.2004.06.002

Qi, G., & Guan, W. (2019). Quantitatively mining and distinguishing situational discomfort grading patterns of drivers from car-following data. *Accident Analysis & Prevention*, *123*, 282–290. Retrieved from https://doi.org/10.1016/j.aap.2018.12.006

Saifuzzaman, M., & Zheng, Z. (2014). Incorporating human-factors in car-following models: a review of recent developments and research needs. *Transportation research part C: emerging technologies*, *48*, 379–403. Retrieved from https://doi.org/10.1016/j.trc.2014.09.008

Sheng, S., Pakdamanian, E., Han, K., Wang, Z., & Feng, L. (2022). A study on learning and simulating personalized car-following driving style. In *2022 ieee 25th international conference on intelligent transportation systems (itsc)* (pp. 1208–1215). Retrieved from https://doi.org/10.1109/ITSC55140.2022.9922548

Summala, H. (2007). Towards understanding motivational and emotional factors in driver behaviour: Comfort through satisficing. In *Modelling driver behaviour in automotive environments* (pp. 189–207). Springer. Retrieved from https://link.springer.com/content/pdf/10.1007/978-1-84628-618-6.pdf?pdf=button

Tao, P., Wang, D., Jin, S., & Ma, D. (2011). A car-following model based on the distribution characteristic of headway. In *Icctp 2011: Towards sustainable transportation systems* (pp. 1368–1378). Retrieved from https://doi.org/10.1061/41186(421)136

Van der Maaten, L., & Hinton, G. (2008). Visualizing data using t-sne. *Journal of machine learning research*, *9*(11). Retrieved from https://www.jmlr.org/papers/volume9/vandermaaten08a/vandermaaten08a.pdf?fbcl

Wang, K., Yang, Y., Wang, S., & Shi, Z. (2022). Research on car-following model considering driving style. *Mathematical Problems in Engineering*, *2022*. Retrieved from https://doi.org/10.1155/2022/7215697

Wang, W., Wang, Y., Liu, Y., & Wu, B. (2021). An empirical study on heterogeneous traffic car-following safety indicators considering vehicle types. *Transportmetrica A: Transport Science*, 1–24. Retrieved from https://doi.org/10.1080/23249935.2021.2015475

Wang, Z., Huang, H., Tang, J., Meng, X., & Hu, L. (2022). Velocity control in car-following behavior with autonomous vehicles using reinforcement learning. *Accident Analysis & Prevention*, *174*, 106729. Retrieved from https://doi.org/10.1016/j.aap.2022.106729

Yuan, K., Laval, J., Knoop, V. L., Jiang, R., & Hoogendoorn, S. P. (2018). A geometric brownian motion car-following model: towards a better understanding of capacity drop. *Transportmetrica B: Transport Dynamics*. Retrieved from https://doi.org/10.1080/21680566.2018.1518169

Zhang, Y., Chen, X., Wang, J., Zheng, Z., & Wu, K. (2022). A generative car-following model conditioned on driving styles. *Transportation Research Part C: Emerging Technologies*, *145*, 103926. Retrieved from https://doi.org/10.1016/j.trc.2022.103926

Zhang, Y., Ni, P., Li, M., Liu, H., & Yin, B. (2017). A new car-following model considering driving characteristics and preceding vehicle's acceleration. *Journal of advanced transportation*, *2017*. Retrieved from https://doi.org/10.1155/2017/2437539

Zhu, M., Wang, Y., Pu, Z., Hu, J., Wang, X., & Ke, R. (2020). Safe, efficient, and comfortable velocity control based on reinforcement learning for autonomous driving. *Transportation Research Part C: Emerging Technologies*, *117*, 102662. Retrieved from https://doi.org/10.1016/j.trc.2020.102662